Development of a Premixed Combustion Capability for Scramjet Combustion Experiments

Robert D. Rockwell[1], Christopher P. Goyne[2], Brian E. Rice[3], Harsha Chelliah[4], James C. McDaniel[5],
University of Virginia, Charlottesville, Virginia, 22904

Jack R. Edwards[6]
North Carolina State University, Raleigh, NC 27695

Luca M. L. Cantu[7], Emanuela C. A. Gallo[8], Andrew D. Cutler[9]
The George Washington University, Waashington, DC, 20052

and

Paul M. Danehy[10]
NASA Langley Resaearch Center, Hampton, VA, 23681

Hypersonic air-breathing engines rely on scramjet combustion processes, which involve high speed, compressible, and highly turbulent flows. The combustion environment and the turbulent flames at the heart of these engines are difficult to simulate and study in the laboratory under well controlled conditions. Typically, wind-tunnel testing is performed that more closely approximates engine testing rather than a careful investigation of the underlying physics that drives the combustion process. The experiments described in this paper, along with companion data sets being developed separately, aim to isolate the chemical kinetic effects from the fuel-air mixing process in a dual-mode scramjet combustion environment. A unique fuel injection approach is taken that produces a nearly uniform fuel-air mixture at the entrance to the combustor. This approach relies on the precombustion shock train upstream of the dual-mode scramjet combustor. A stable ethylene flame anchored on a cavity flameholder with a uniformly mixed combustor inflow has been achieved in these experiments allowing numerous companion studies involving coherent anti-Stokes Raman scattering (CARS), particle image velocimetry (PIV), and planar laser induced fluorescence (PLIF) to be performed.

I. Introduction

Sustained hypersonic flight via scramjet propulsion presents considerable capabilities for future space access and high speed weapons. However, in order for this technology to become a practical and reliable propulsion method, there is a need for improved understanding and prediction of the reacting flow of the scramjet combustor, which is highly compressible and highly turbulent. The fundamental processes in the combustor include the injection, mixing, and reaction of a fuel in a supersonic or high speed airstream. For certain fuels, such as hydrogen,

---

[1] Senior Scientist, Mechanical and Aerospace Engineering, Member AIAA.
[2] Associate Professor, Mechanical and Aerospace Engineering, Associate Fellow AIAA.
[3] Graduate Research Assistant, Mechanical and Aerospace Engineering, Member AIAA.
[4] Professor, Mechanical and Aerospace Engineering, Member AIA.
[5] Professor, Mechanical and Aerospace Engineering, Associate Fellow AIAA.
[6] Professor, Mechanical and Aerospace Engineering, Associate Fellow AIAA.
[7] Ph.D. Candidate, Mechanical and Aerospace Engineering, Member AIAA
[8] Ph.D. Candidate, Mechanical and Aerospace Engineering, Member AIAA
[9] Professor, Mechanical and Aerospace Engineering, Associate Fellow AIAA.
[10] Research Scientist, Advanced Measurements and Data Systems Branch, Associate Fellow AIAA.

the chemical kinetic time scales are much shorter than the flow time scales, and the rate-controlling process is the fuel-air mixing. While hydrocarbon fuels have longer kinetic time scales than hydrogen, the mixing can still be rate-controlling if the flow temperature is high or if a flameholder is present and there is an adequate source of combustion radicals. In order to focus on a process that is fundamental to scramjet combustion, the present study examines high speed premixed fuel-air flows. In this way, the mixing may be decoupled from the turbulent combustion and the chemical kinetics become rate-controlling. This allows the turbulent combustion physics to be isolated. Models of turbulence-chemistry closures can then be developed and validated. Investigations of the effect of turbulent fluctuations on flame structure, including eddy sizes and distributions, can also be conducted. Furthermore, complications, such as the effect of jet mixing on flame propagation, can be avoided.

Unlike in non-premixed turbulent combustion, where there is no meaningful time scale based on velocity, in premixed turbulent combustion the velocity fluctuations, v', play a critical role in defining the turbulent combustion regimes. For low density ratio variations, the dependence of normalized turbulent velocity fluctuations with respect to laminar burning velocity, v'/s_L, to the normalized integral turbulent length, l/l_L are well established, and are given by

$$\frac{v'}{s_L} = Re_l \left(\frac{l}{l_L}\right)^{-1},$$
$$= Da_l^{-1} \left(\frac{l}{l_L}\right),$$
$$= Ka_\eta^{2/3} \left(\frac{l}{l_L}\right)^{1/3},$$

$$(1)$$

where Re_l is the Reynolds number based on integral length scale, Ka_η is the Karlovitz number based on Kolmogorov length scale, and Da_l is the Damkohler number based on integral length scale [1]. For large Re_l numbers, the above relationships yield four distinct turbulent combustion regimes identified as wrinkled flamelets, corrugated flamelets, distributed reaction zones, and well-stirred reaction zones [2]. It is currently not known in which regime a scramjet with premixed combustion operates. Therefore, a high speed premixed combustion capability is desirable in order to conduct experiments to identify the combustion regime of these flames.

For scramjet combustion that involves turbulent compressible reacting flows with large density variations, the turbulent combustion regimes are influenced by an additional parameter characterized by

$$S = \Delta T_s / \Delta T_c,$$

$$(2)$$

where ΔT_s is the change in temperature associated with kinetic energy and ΔT_c is the change in temperature associated with the chemistry [3]. If the rise in temperature associated with kinetic energy is approximated by

$$\Delta T_s = (1/2)(\gamma - 1)\bar{M}^2 T_0,$$

$$(3)$$

then the parameter S becomes

$$S = \frac{1}{2}(\gamma - 1)\bar{M}^2 \frac{T_0}{\Delta T_c},$$

$$(4)$$

where $\Delta T_c / T_0$ can be identified as a heat release parameter, α, with typical values ranging from 1 to 10 [4]. If typical values of $\alpha = 6$ and $\gamma = 1.3$ are selected, then M = 6 flow yields $S = 1$, indicating that velocity fluctuations can introduce temperature fluctuations close to the increase in temperature by chemical reactions. This demonstrates how closely coupled velocity fluctuations and chemical reactions can be in the high speed combustion environment of a scramjet. By decoupling the mixing from the turbulent combustion process, the experiments described in this paper offer an opportunity to examine the turbulence-chemistry coupling in a scramjet relevant environment.

Therefore, the main goal of the present research is to develop a high speed premixed combustion capability to enable investigation of the strong coupling between flow compressibility, turbulence, and heat release. By applying advanced diagnostics, the exact turbulent combustion regime of the scramjet combustor may be identified. Such measurements have not been previously published for scramjet combustors nor has stable high speed premixed combustion been demonstrated. The specific objectives of the present study are: 1) design and construct fuel-air

premix hardware for a series of high speed combustion experiments, 2) demonstrate stable premixed combustion in a scramjet combustor, and 3) examine the effects of equivalence ratio and inflow gas temperature on flame ignition, propagation, and flameout.

This study is part of a larger effort of the National Center for Hypersonic Combined Cycle Propulsion (NCHCCP) that is aimed at examining combustion in a dual-mode scramjet with flight Mach numbers in the range of 4 to 6. Here, a theoretical flight vehicle would be expected to transition from a subsonic ramjet mode of combustion to a supersonic scramjet mode of combustion. As part of this larger effort, a suite of advanced instream diagnostics are available including coherent anti-Stokes Raman scattering (CARS), OH and CH_2O planar laser induced fluorescence (PLIF), and particle image velocimetry (PIV) [5-7]. Together with conventional measurement techniques, these diagnostics enable the study of both the cavity flow (operability limits, residence time, internal cavity flame structure, and shear layer characterization) and the main flame (flame surface area, local strain rate/stretch and flame propagation angle). The experiments described in this paper have resulted in databases that are currently under development and, through collaboration with the NCHCCP, are leading to the validation of advanced time averaged and time accurate numerical models [8]. Details and status of the CARS and PIV measurements are presented elsewhere by Gallo and Kirik, respectively [9,10]. Edwards presents results of the numerical modeling efforts [11]. The purpose of this paper is to report on the development and demonstration of the premixed capability and the initial experimental results.

II. Experimental Approach

Three focus areas have been identified to guide the experimental approach: 1) measurement of reacting flow turbulence statistics and novel fuel-air mixing and flameholding schemes through the development and application of advanced diagnostics, 2) development of benchmark data sets with quantified experimental uncertainty for the purposes of developing accurate RANS, hybrid LES/RANS, and LES computational models, and 3) generation of performance improvements of combined cycle systems and the development of methods for controlling combined cycle mode-transition [12].

The dual-mode scramjet experiments are being conducted with the aim of examining the flow processes that take place in the isolator and combustor in the flight Mach number regime of 4 to 6. Specifically, the experiments employ a direct connect scramjet combustor that is operated at Mach 5 enthalpy (total temperature of 1200 K) using the University of Virginia Supersonic Combustion Facility (UVaSCF). The test-section hardware has been designed to accommodate the application of multiple advanced flow diagnostic techniques [13]. In particular, the combustor section incorporates a modular construction approach that provides substantial access for optical laser diagnostics. In addition to static wall pressure and temperature measurements, a number of advanced, instream diagnostics have been applied in the facility, including CARS, OH PLIF (Hz), CH_2O PLIF (Hz and kHz), stereoscopic and planar PIV (Hz and kHz), and high speed chemiluminescence imaging (Hz and kHz). Combined, these diagnostics result in the measurement of: wall static pressure, temperature, species concentration (N_2, O_2, H_2, CO, CO_2, H_2O, C_2H_4, and qualitative OH), scalar correlations, three-component velocity, three-component turbulence intensity (RMS), and Reynolds stresses.

The experiments described in this paper have used ethylene fueling in what is termed the modified Configuration E (Fig. 1). The flowpath starts with a Mach 2 facility nozzle and incorporates a long, constant-area isolator upstream of the combustor that contains any precombustion shock train. Injecting fuel at the upstream end of the isolator allows for significant mixing of the fuel into the freestream ahead of the cavity flameholder. The isolator is a 15.97" long rectangular duct with a 1" x 1.5" cross-section. A 2.9° divergence on the cavity-side wall starts 2.1" upstream of the cavity leading edge. This divergence is maintained through the combustor and extender sections of the flowpath. A constant area section downstream of the combustor compresses the flow inducing a thermal throat when the flowpath is operating in the dual-mode with a precombustion shock train in the isolator and subsonic flow through the combustor. CFD analysis indicates this feature promotes flameholding in the combustor. The cavity spans the width of the duct and has an initial depth of 0.356", which is maintained over a length of 1.22". The cavity closes with a 22.5° ramp that terminates 2.1" downstream of the leading edge. The scramjet terminates with an atmospheric backpressure at the exit, 19.61" downstream of the cavity leading edge. The exit of the combustor is 40.8" from the exit of the Mach 2 nozzle.

All components in the flowpath were constructed of stainless steel with the exception of the cavity wall of the combustor, which is OFHC copper, and the large optical windows in the combustor, which are 0.375" thick fused-silica. Water cooling is incorporated in each component of the test-section and all stainless steel walls in the isolator, combustor, and constant area section are coated with a 0.015" thick layer of thermal barrier zirconia. The copper cavity wall is not coated.
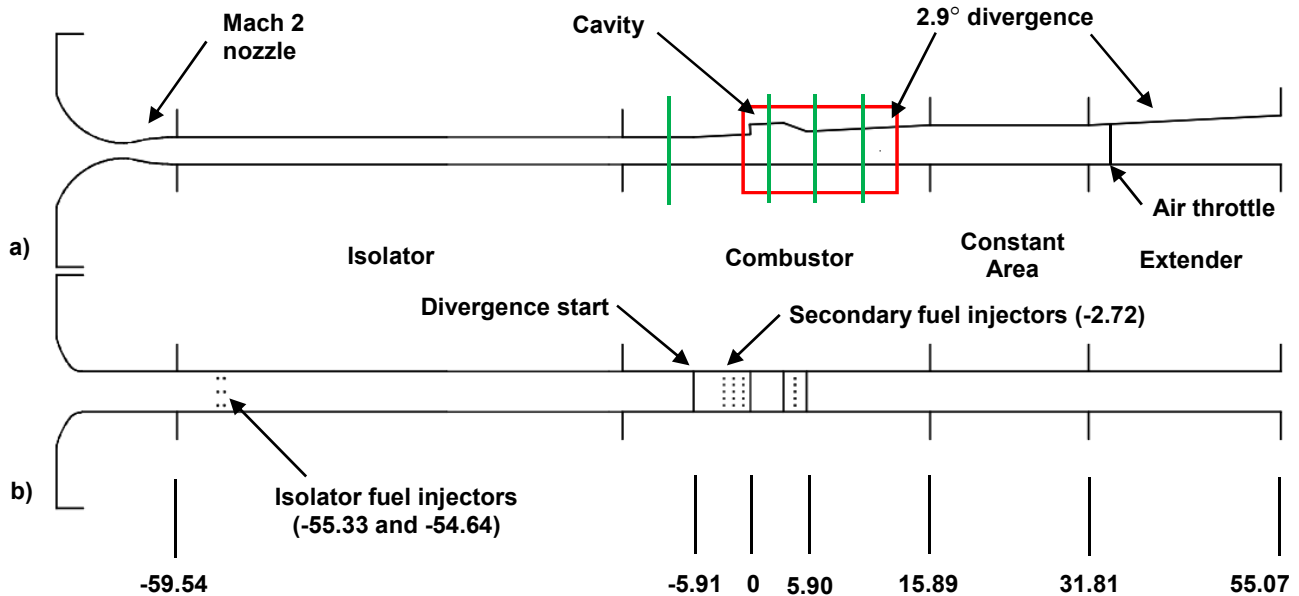
Figure 1. Modified Configuration E flowpath showing CARS measurement planes (green) and OH PLIF field of view (red): a) side view and b) top view with normalized axial distances from cavity leading edge (x/h).

The primary measurement locations are indicated in Fig. 1. Nitric oxide (NO) PLIF measurements were taken at the leading edge of the cavity to verify the level of premixing. Other measurements taken in this flowpath but not reported here include CARS, PLIF (OH and CH_2O), and PIV. The vertical green lines in Fig. 1 represent the CARS measurement locations. Normalized by the cavity depth (h = 0.356"), these measurement planes are at axial locations of x/h = -9.14, 2.39, 6.60, and 10.80 relative to the cavity leading edge. PLIF (OH and CH_2O) has been performed from the cavity leading edge to the downstream end of the optical windows in the duct, as indicated by the red box in Fig. 1. The cavity-side wall is instrumented from inlet to exit with 80 low frequency pressure taps and 13 type K thermocouples that are primarily located on the combustor centerline.

III.   Facility and Flow Conditions

The experiments were conducted using the UVaSCF. This facility is an electrically heated, continuous flow, direct-connect scramjet wind tunnel. It is capable of simulating up to Mach 5 flight enthalpy and provides a clean test flow that is free of contaminates such as those from a vitiation heater. Facility run times are on the order of hours with steady-state heating and fuel conditions. Because CARS is a point-by-point measurement technique, the extended run time provides for high spatial resolutions using a finely-spaced measurement grid [5]. Likewise, PIV and PLIF require non-correlated image counts on the order of 500 to 1000 or more for calculating average turbulence statistics and other parameters to a reasonable degree of accuracy [7,14,15]. Coupled with the optical access in the tunnel and proximity to laser diagnostics labs, the facility is well suited to the application of the advanced optical diagnostics required by the NCHCCP.

The facility flow conditions are presented in Table 1. The uncertainies given in the table are calculated by standard propagation of error and include temporal variability as well as instrumentation uncertainty. Tunnel air flow conditions were typically maintained to less than ±1% during a run and across multiple runs. The facility is fully described elsewhere [16-18].

An air throttle is available downstream of the combustor, near the upstream end of the extender (at x/h = 37.52), which allows the duct to be back pressured independently or in conjunction with a combustion process to simulate the pressure rise associated with combustion. The throttle consists of two slotted, high pressure air injectors, one in each side wall, that are used to restrict flow at that location. The slots are 0.125" wide and extend over the full height of the duct. Although air throttle pressures and flow rates are not generally measured directly, the isolator pressures were monitored in real time with adjustments made to the throttle to maintain the desired shock location. Through use of the air throttle, it is possible to accurately locate and stabilize the leading edge of the isolator shock train at any point in the duct.

Table 1. Test conditions for main air flow.

Parameter	Air	Uncertainty
Total pressure (kPa)	300	± 1%
Total temperature (K)	1200	± 0.8%
Mach number[*]	2.03	± 1%

[*] Property at nozzle exit determined using nozzle area ratio and assuming isentropic flow (γ=1.36 for air).

A NetScanner[TM] pressure scanner and remote NetScanner[TM] thermocouple unit were used to acquire wall pressures and temperatures along the centerline of the fuel injector wall in the scramjet flowpath. Typically, a scan of 20 samples was acquired over 2 seconds at a sample rate of 10 Hz for each pressure tap and thermocouple. This data was then averaged and normalized by the measured pressure at the most upstream pressure tap (located 0.25 in. downstream of the facility nozzle exit) prior to plotting. Wall pressure and temperature were typically measured to within ±0.5% and average quantities had a 95% confidence interval of no more than ±1.5%.

IV. Fuel Injection and Mixing

As indicated in Fig. 1b, the primary ethylene fuel injection is through two banks of six sonic, flush-wall injectors located at the upstream end of the isolator, 1.5 inches downstream of the facility nozzle exit on opposite walls of the duct. Injection at this location allows the fuel to be processed by the isolator shock train ideally resulting in a fully premixed flow at the cavity leading edge. Each bank comprises two rows of three equally spaced 0.049 inch diameter injectors oriented normal to the freestream flow. The total fuel pressure and temperature for each set of injectors is monitored and controlled to provide the desired fuel split and flow rate.

Table 2 lists the primary fueling conditions used in these experiments. As will be discused later, the first fuel condition represents the maximum fuel rate that can be accommodated by the flowpath without unstarting the isolator. The second fuel condition is close to the lean flameout point of the flowpath with a fully premixed combustor inflow. There is a difference in the fuel injection pressures between the cavity-side bank and the opposite-side bank, which is due to a small difference in the discharge coefficients of the two injector banks (0.60 for the cavity-side bank and 0.56 for the opposite-side bank). Control valves in the fuel system allow the fuel to be evenly split between the two injector banks as shown in Table 2 or adjusted such that a larger proportion of fuel is delivered through the cavity-side injector bank. Also shown in Fig. 1b, a secondary fuel injection location is through a row of five equally spaced 0.021 inch diameter sonic, flush-wall injectors located 0.97 inches upstream of the cavity leading edge. The secondary injectors are too close to the cavity for the fuel injected through them to fully mix with the freestream and instead provide a means for more directly fueling the cavity. This allows the flowpath to operate in the scram mode with either a short or nonexistent precombustion shock train.

Table 2. Test conditions for ethylene fuel.

Parameter	Fuel Condition 1		Fuel Condition 2		Uncertainty
	Cavity-Side	Opposite-Side	Cavity-Side	Opposite-Side	
Equivalence ratio	0.20	0.20	0.17	0.17	± 5%
Total pressure (kPa)	260	270	207	223	± 3%
Total temperature (K)	288	288	288	288	± 3%
Mach number[*]	1.0	1.0	1.0	1.0	± 0.5%

[*] Property at nozzle exit determined using nozzle area ratios and assuming isentropic flow (γ=1.36 for air, 1.24 for C_2H_4).

The static fuel temperatures listed in Table 2 are below the autoignition temperature of ethylene. However, following ignition by an outside source, the flame is self-sustaining. Ignition is achieved by using the air throttle to pressurize the cavity while injecting hydrogen through a port in the base of the cavity. Under these conditions the hydrogen autoignites and ethylene fuel can then be introduced through the upstream injectors. Once a sufficient flow

rate of ethylene is established (typically a global fuel equivalence ratio greater than 0.33), the hydrogen can be turned off. The air throttle may be maintained or not depending on the nature of the particular experiment being performed.

NO PLIF measurements were used to evaluate the level of fuel premixing at the leading edge of the cavity. A mixture of 10% (molar) NO in nitrogen was used as a surrogate for the ethylene fuel. Note that combustion by-products, such as OH or C*, are not present upstream of the combustion region. Importantly, the molar weight of this NO/N_2 gas mixture is nearly identical to that of ethylene, which allows the fuel system operation, including injection pressures, to be the same for equivalent mass flow rates of NO and ethylene. With no combustion process present, the air throttle was used to generate a combustor back pressure equivalent to that due to combustion at a given fuel equivalence ratio and thus drive the isolator shock train. A full description of the NO PLIF measurements is given elsewhere [15].

Uniform fuel premixing for the case with both banks of isolator injectors operating and a precombustion shock train in the isolator has been confirmed with NO PLIF as shown in Fig. 2. Figure 2a is a single-shot instantaneous image and Fig. 2b shows the average distribution. These images present a qualitative representation of the fuel distribution at the cavity leading edge and, within the uncertainty of the NO PLIF measurement, represent an essentially uniform fuel-air mix.

For comparison, Fig. 3 shows the fuel distribution from a single isolator fuel injector located on the centerline of the cavity-side wall with no shock train to promote mixing. In this case, the dark region along the lateral edges and on the wall opposite the active fuel injector shows that NO has not propogated to fill the duct.
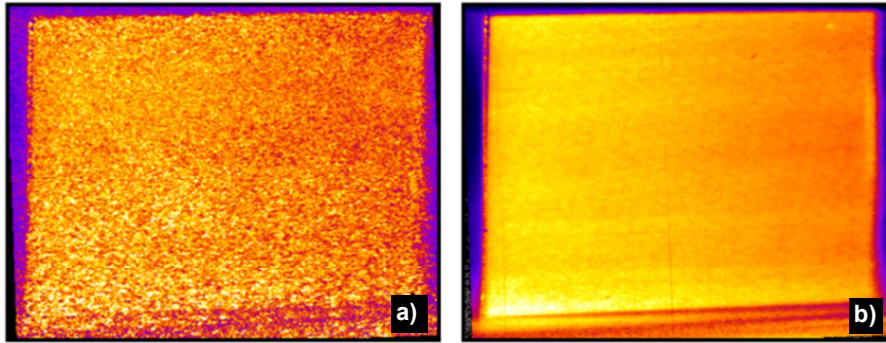

Figure 2: Instantaneous (a) and averaged (b) NO PLIF images of fuel simulant distribution for two rows of fuel injection from both walls with global equvalence ratio = 0.42 and shock train leading edge at x/h = -45 (adapted from [15]).
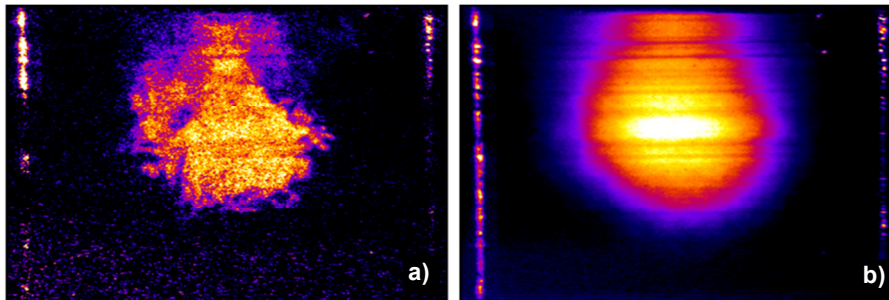

Figure 3: Instantaneous (a) and averaged (b) NO PLIF images of fuel simulant distributions for a single fuel injector with equivalence ratio = 0.09 and no shock train (adapted from [15]).

V.   Results

Figures 4 and 5 show the axial distribution of static pressure on the cavity-side wall for global fuel equivalence ratios, φ, of approximately 0.40 and 0.34, respectively. The measured pressures have been normalized by the static pressure at the exit of the facility nozzle, P_{ref}, and the axial locations are normalized by the cavity depth (0.356 in.). The cavity leading edge is at x/h = 0. Results for the case with all fuel being delivered through the cavity-side bank of injectors are shown along with two different fuel split ratios. The solid square symbols represent an equal fuel split between the cavity-side injector bank and the opposite-side injector bank. This fueling scenario is equivalent to

that shown in Fig. 2 above and represents a uniform fuel-air premix. Also shown in the figures are the pressure distributions for the NO PLIF measurements, represented by a dashed line. In these cases the air throttle, rather than a combustion process, was used to generate the back pressure that drives the shock train in the isolator. It can be seen that the pressure rise in the isolator is the same whether it is due to a combustion process or the air throttle giving confidence in the NO PLIF mixing study. The fuel off case is also shown for reference.
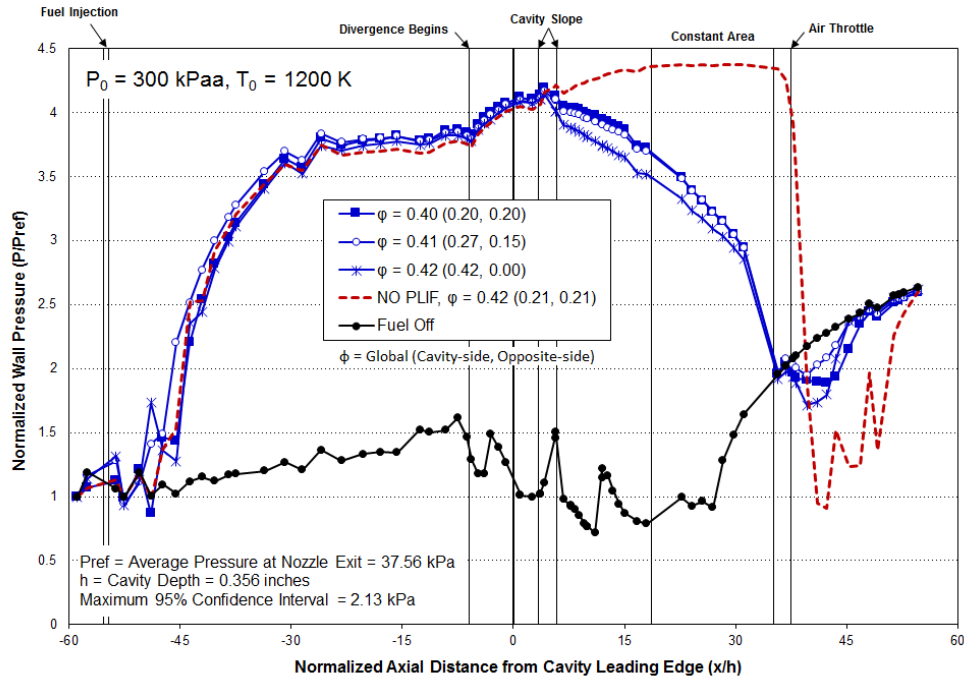
Figure 4. Normalized wall pressures at fuel condition 1. In the legend, the numbers in parentheses indicate the cavity-side and opposite-side fuel equivalence ratio, respectively.
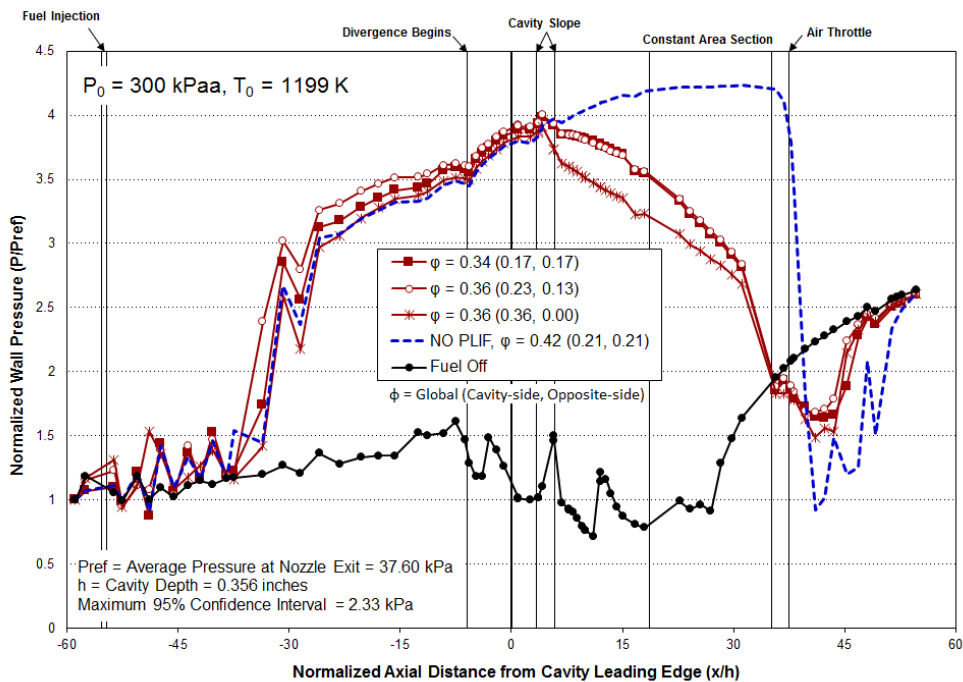

Figure 5. Normalized wall pressures at fuel condition 2. In the legend, the numbers in parentheses indicate the cavity-side and opposite-side fuel equivalence ratio, respectively.

7

American Institute of Aeronautics and Astronautics

For both global fuel equivalence ratios, delivering all of the fuel through the cavity-side injectors alone will result in some level of fuel stratification across the duct with a higher density of fuel on the cavity-side wall. All fuel conditions shown in Figs. 4 and 5 result in a stable dual-mode scramjet flame anchored on the cavity that can be maintained for one to two hours in this facility with depletion of the fuel tanks being the limiting factor.

It can be seen that while the pressures in the isolator and onset of the precombustion shock train are nearly the same for all three fuel splits, pressures are noticeably different in the combustor section between the cavity and the thermal throat (from $x/h = 5$ to 35). Here, the flow is subsonic in a one-dimensional sense and heat released in the flame drives the pressure down. It is evident that the stratified cases, with all the fuel delivered through the cavity-side injector bank, results in an initially steeper drop in pressure in the vicinity of the cavity closeout ramp ($x/h = 5$), perhaps due to more robust combustion in the vicinity of the cavity. However, the more uniformly mixed cases result in higher combustor pressures overall and presumably would generate more thrust.

All of the fueled cases shown in Figs. 4 and 5 represent operation of the scramjet flowpath in the dual-mode with separated flow and a precombustion shock train in the isolator. Using a one-dimensional model of the separated flow in the isolator [19], the one-dimensional Mach number at the cavity leading edge is estimated to be 0.70 for the $\varphi = 0.40$ case and 0.72 for the $\varphi = 0.34$ case. A thermal throat can be seen at the downstream end of the constant area section ($x/h = 35$), which represents the transition back to supersonic flow and indicates that the combustion process is isolated from the atmospheric back pressure. Note that at global fuel equivalence ratios above 0.4, the leading edge of the precombustion shock train is approaching the isolator fuel injection location. Care must be taken during these experiments to avoid impingement of the shock train directly on the fuel injectors as that results in ignition of the fuel in the isolator leading to a large pressure spike in the flowpath and likely damage or breakage of the windows. Thus, to provide some margin and avoid damaging tunnel hardware, a practical upper fueling limit for continuous testing is a global equivalence ratio of 0.42 with an absolute upper bound of 0.45.

An important aspect of these experiments was to determine the limits of operability of the flowpath. As mentioned above, the upper limit on equivalence ratio has been determined to be 0.45 to avoid impingement of the shock train on the upstream fuel injectors. In order to determine the lower flameholding limits, a number of lean and low temperature flameout tests were performed by slowly lowering either the fuel flow rate (lean flameout) or heater temperature (low temperature flameout) until the flame was no longer sustained. Figure 6 shows the results of these tests with each data point representing an observed flameout. Although there is some variability in the data, flameout consistently occurs at a global equivalence ratio just above 0.3 when the total temperature is 1200 K. Thus, the maximum range of equivalence ratio is about 0.14 or a little over 30%. At lower temperatures between 1000 K and 1100 K, the fuel equivalence ratio required to sustain combustion rises to between 0.35 and 0.39 resulting in a range of operability of only 0.06 or 15%. Additional tests were performed with the air throttle on to provide additional back pressure such that the leading edge of the precombustion shock train was maintained at $x/h = -45$. At a total temperature of 1200 K, the incremental increase in static temperature behind the longer shock train sustains combustion down to an equivalence ratio between 0.26 and 0.29. This represents approximately 10% less fuel than with the air throttle off and gives an operability range in equivalence ratio of 0.16 to 0.19, which is between 40% and 50%.

Figures 7 is an instantaneous, high speed chmiluminescence image taken at a global equivalence ratio of 0.41 with approximately 2/3 of the fuel from the cavity-side injector bank and 1/3 from the opposite-side bank. Figure 8 is the same image taken at a global equivalence ratio of 0.31. The chemiluminescence is primarily due to emission from excited CH in the active reaction zone. Both images were taken with a 0.6 ms exposure. At both equivalence ratios, the flame is anchored on the cavity with combustion initiating along the shear layer between the cavity and the freestream air, impinges on the sloped cavity closeout surface, and propogates downstream expanding away from the cavity-side wall. There is little to no chemiluminescence near the cavity leading edge in either case. As would be expected, the higher fuel rate results in a somewhat more robust and brighter flame. The field of view is limited to 6.6 cavity depths (2.35 inches) downstream of the cavity leading edge and at that point the flame propagates a little over halfway across the duct in Fig. 7 and little less than halfway in Fig. 8.

Figure 9 illustrates scramjet mode transition from a purely scram mode of operation with no pressure rise upstream of the cavity to the dual-mode discussed above. In this test, the fuel was delivered through both the primary fuel injectors in the isolator as well as the secondary injectors immediately upstream of the cavity. Only the cavity-side injectors in the isolator were used. The lower equivalence ratios (seen in blue) represent the purely scram mode of operation with no pressure rise upstream of the cavity and a one-dimensional Mach number of 1.49 at the leading edge of the cavity leading. Using a combination of the primary and secondary injectors in this fashion ensures some proportion of fuel-air premixing. However, the slope of the pressure curves in the combustor are more similar to that of the stratified fuel cases than the fully premixed cases in Figs. 4 and 5. Nevertheless, the data show that the facility and flowpath are capable of supporting scramjet mode transition with ethylene fueling.
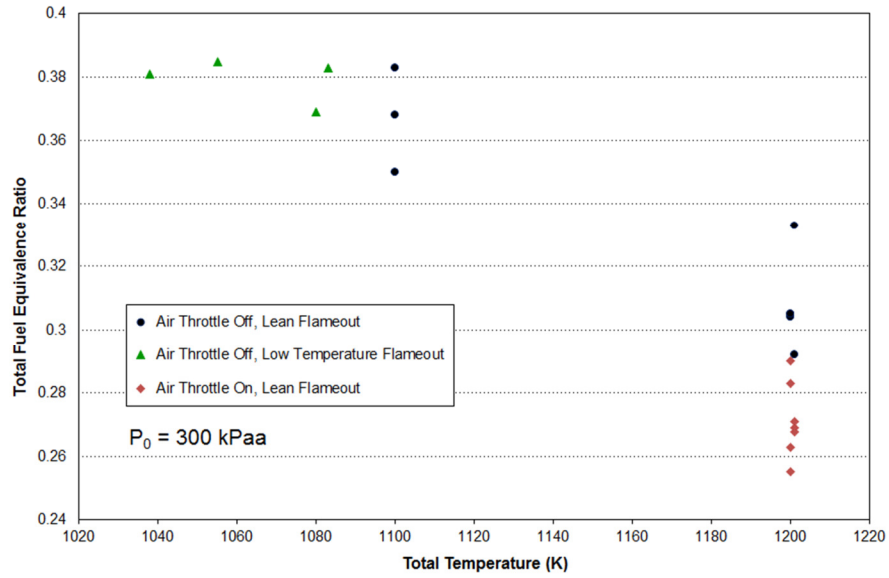
American Institute of Aeronautics and Astronautics

Figure 6. Lean and low temperature flameout points.
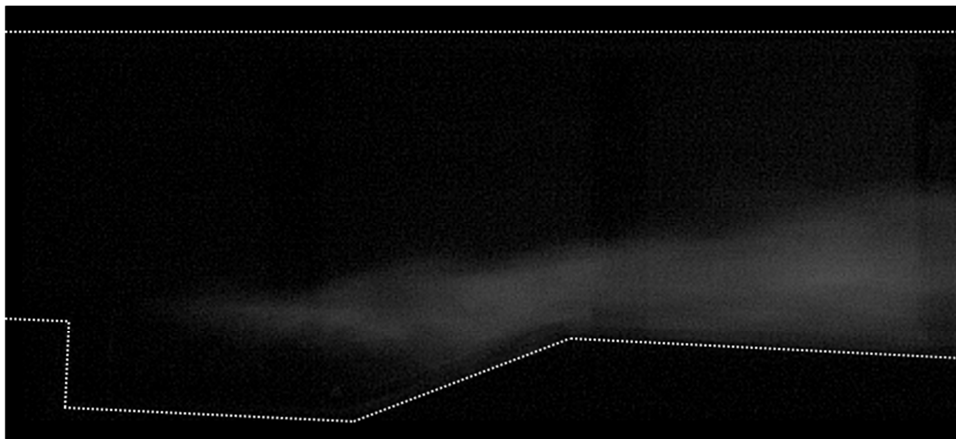

Figure 7. Chemiluminescecnce image (0.6 ms capture) at global φ = 0.41 (cavity-side = 0.27, opposite-side = 0.15).
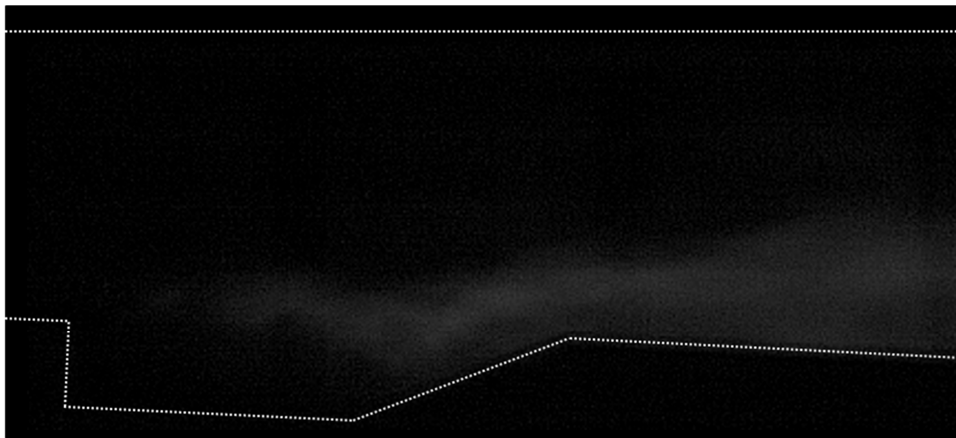

Figure 8. Chemiluminescecnce image (0.6 ms capture) at global φ = 0.31 (cavity-side = 0.20, opposite-side = 0.11).
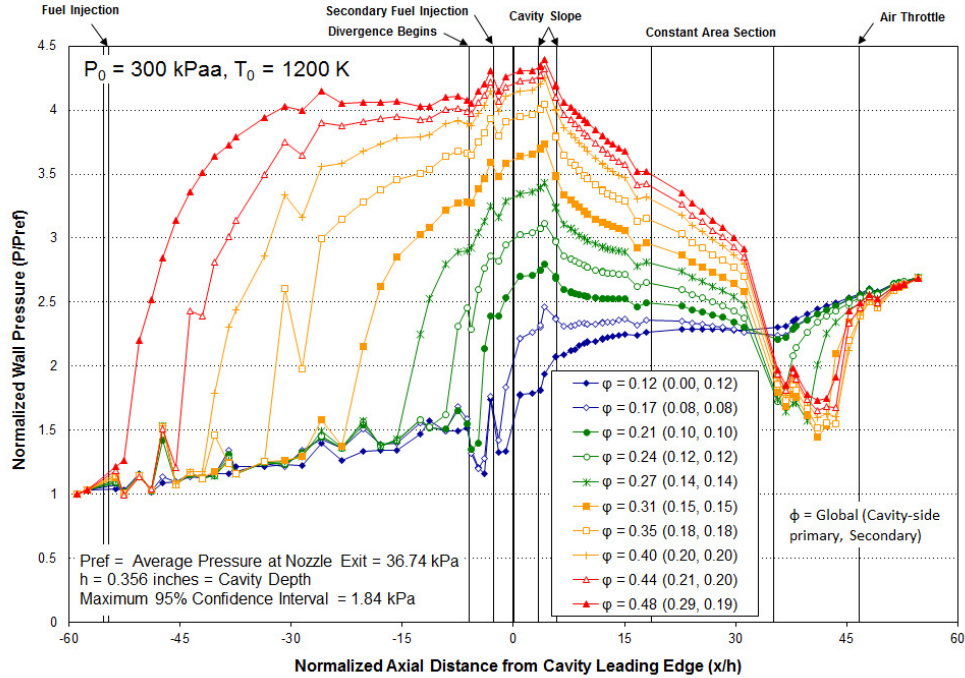
9

Figure 9. Normalized wall pressures illustrating mode transition with primary and secondary fuel injection. In the legend, the numbers in parentheses indicate the primary (cavity-side) and secondary fuel equivalence ratio, respectively.

VI. Conclusion

This paper documents the development of a dual-mode scramjet flowpath and fuel injection scheme that is capable of sustaining a high speed, uniformly premixed, turbulent flame with a combustor inlet Mach number of about 0.7. The work relies on a precombustion shock train in the isolator to enhance the fuel-air mixing. The resulting fuel-air premix uniformity at the leading edge of the cavity flameholder has been verified with NO PLIF. Furthermore, the flowpath is also capable of supporting a purely scram mode of combustion with no precombustion shock train as well as a transitional scram mode with a short shock train and supersonic combustor inflow.

Within the operability limits of the flowpath documented in this paper, the scramjet flame is stably anchored on the cavity and is highly repeatable. This presents a suitable test environment for time-intensive diagnostics such as fine-grid CARS as well as PLIF and PIV, which can be performed in sufficient quantity to yield statistically meaningful quantitive results.

Acknowledgments

References

[1] Peters, N., *Turbulent Combustion*, Cambridge University Press, 2000.

[2] Borghi, R., "Turbulent Combustion Modeling," *Progress in Energy and Combustion Science*, Vol. 14, No. 4, 1988, pp. 245-292.

[3] Bray, K., Libby, P.,Williams, F., High Speed Turbulent Combustion in *Turbulent Reacting Flows* (eds. Libby, P.A. and Williams, F.A.), Academic Press, London, UK, 1994.

[4] Williams, F.A., *Combustion Theory*, Westview Press, 1985.

[5] Cutler, A.D., Magnotti, G., Cantu, L., Gallo, E., Rockwell, R.D., and Goyne, C.P., "Dual-Pump Coherent Anti-Stokes Raman Spectroscopy Measurements in a Dual-Mode Scramjet," *Journal of Propulsion and Power*, Vol. 30, No. 3, 2014, pp. 539-549.

[6] Johansen, C.T., McRae, C.D., Danehy, P.M., Gallo, E.C., Cantu, L.M., Magnotti, G., Cutler, A.D., Rockwell, R.D., Goyne, C.P., and McDaniel, J.C., "OH PLIF of Uva Supersonic Combustion Experiment: Configuration A," *Journal of Visualization,* Vol. 17, No. 2, 2014, pp. 131-141.

[7] Rice, B.E., Goyne, C.P., McDaniel, J.C., and Rockwell, R.D., "Characterization of a Dual-Mode Scramjet via Stereoscopic Particle Image Velocimetry," AIAA 2014-0986, 52nd AIAA Aerospace Sciences Meeting, National Harbor, MD, Jan. 2014.

[8] Fulton, J.A., Edwards, J.R., Hassan, H.A., McDaniel, J.C., Goyne, C.P., Rockwell, R.D., Cutler, A.D., Johansen, C.T., and Danehy, P.M., "Large-Eddy/Reynolds-Averaged Navier-Stokes Simulations of Reactive Flow in Dual-Mode Scramjet Combustor," *Journal of Propulsion and Power*, Vol. 30, No. 3, 2014, pp. 558-575.

[9] Gallo, E.C., Cantu, L.M., Cutler, A.D., Danehy, P.M., Rockwell, R.D., Goyne, C.P., and McDaniel, J.C., Oral Presentation: Coherent Anti-Stokes Raman Spectroscopy (CARS) in a Dual-Mode Scramjet with Premixed Fueling, 53rd AIAA Aerospace Sciences Meeting, Kissimmee, FL, Jan. 2015.

[10] Kirik, J.W., Goyne, C.P., McDaniel, J.C., Rockwell, R.D., Johnson, R.F., and Chelliah, H.K., "Velocimetry Using Graphite Tracer Particles in a Scramjet Flowpath," 53rd AIAA Aerospace Sciences Meeting, Kissimmee, FL, Jan. 2015.

[11] Kumar, K., Edwards, J.R., Goyne, C.P., and McDaniel, J.C., "Large Eddy Simulation of High-Speed, Premixed Ethylene Combustion," 53rd AIAA Aerospace Sciences Meeting, Kissimmee, FL, Jan. 2015.

[12] McDaniel, J.C., Chelliah, H., Goyne, C.P., Edwards, J.R., Givi, P., Cutler, A.D., "US National Center for Hypersonic Combined Cycle Propulsion: An Overview," AIAA-2009-7280, 16th AIAA/DLR/DGLR International Space Planes and Hypersonic Systems and Technologies Conference, Bremen, Germany, Oct 2009.

[13] Rockwell, R.D., Goyne, C.P., Rice, B.E., Kouchi, T., McDaniel, J.C., and Edwards, J.R., "Collaborative Experimental and Computational Study of a Dual-Mode Scramjet Combustor," *Journal of Propulsion and Power*, Vol. 30, No. 3, 2014, pp. 530-538.

[14] Ullum, U., Schmidt, J.J., Larsen, P.S., and McCluskey, D.R., "Statistical Analysis and Accuracy of PIV Data," *Journal of Visualization*, Vol. 1, No. 2, 1998, pp. 205-216.

[15] Cantu, L.M., Gallo, E.C., Cutler, A.D., Bathel, B.F., Danehy, P.M., Rockwell, R.D., Goyne, C.P., and McDaniel, J.C., "Nitric Oxide PLIF Visualization of Simulated Fuel-Air Mixing in a Dual-Mode Scramjet," 53rd AIAA Aerospace Sciences Meeting, Kissimmee, FL, Jan. 2015.

[16] Rockwell, R.D., Goyne, C.P., Haw, W., Krauss, R.H., McDaniel, J.C., and Trefny, C.J., "Experimental Study of Test-Medium Vitiation Effects on Dual-Mode Scramjet Performance and Power," *Journal of Propulsion and Power*, Vol.27, No.5, 2011, pp. 1135-1142.

[17] Krauss, R.H., McDaniel, J.C., Scott J.E., Whitehurst, R.B., Segal, C., Mahoney, G.T., and Childers, J.M., "Unique, clean-air, continuous-flow, high-stagnation-temperature facility for supersonic combustion research," AIAA Paper 88-3059, 1988.

[18] Krauss, R.H. and McDaniel, J.C., "A Clean Air Continuous Flow Propulsion Facility," AIAA Paper 92-3912, 1992.

[19] Heiser, W.H. and Pratt, D.T., *Hypersonic Airbreathing Propulsion*, AIAA Education Series, AIAA, Washington, D.C., 1994, pp. 332-346.

American Institute of Aeronautics and Astronautics